MODELING AND ANALYSIS OF NOVEL SPRING MADE OF COMPOSITE WITH AND WITHOUT MATERIAL PROPERTY GRADING

Saeed Asiri
Mechanical Engineering Department, King Abdulaziz University
Faculty of Engineering, Jeddah, Saudi Arabia.
Contact: sasiri@kau.edu.sa

ABSTRACT: *Springs are one of the most popular means of mechanically storing and issuing energy, and they can be found in a wide variety of machines and products. Most springs are made of metal, and nowadays, there are many new alloys to choose from, but nonmetallic materials, such as the reinforced plastics and ceramics, have been appearing worldwide. This research aims to establish the performance comparison for circular cross-section springs with the same geometry and manufactured with three different materials: steel, composite, and functionally graded material (FGM) under stable loading using finite element analysis. This paper intends to guide mechanical designers in considering different material options for a spring design. As well as to provide a methodology through finite element analysis for selecting the most favorable material option for the application required. The findings of this research show that some feature performances of compression springs made of carbon steel are improved by using FGM and composite materials. Enhanced capabilities include higher load to failure: 1.48 times in an FGM spring and 1.1 times in a composite spring, as well as increased energy storage: 1.53 times in an FGM spring and 6.84 times in a composite spring; and less weight representing only 61% in an FGM spring and 24% in a composite spring.*

Keywords: helical springs, circular cross-section springs, FEA simulation, functionally graded material (FGM), composite material

1. INTRODUCTION

Springs are one of the most popular means of mechanically storing and issuing energy, and they can be found in a wide variety of machines and products. Most springs are made of metal, and nowadays there are many new alloys to choose from, but nonmetallic materials, such as the reinforced plastics and ceramics, have been appearing worldwide. The research aim focuses on contributing to the mechanical design of a spring considering the selection of its manufacturing material. In this sense, it will carry out an analysis of two springs made with two new types of materials used worldwide for manufacturing them, comparing the performance of a spring made of FGM with a spring made of composite materials and these results will be contrasted with a traditional spring made of carbon steel. For completing the evaluation, a finite element analysis will carry out using the commercial software ANSYS Workbench. Three computational cases will perform with the same geometric model of a helical spring of circular cross-section and subjected to compression. It will vary only on the material used in each computational case; for comparing the spring performance made of each of three materials analyzed in this study: FGM, composite material, and carbon steel. First, it will corroborate the computational model of carbon steel spring, comparing the Finite Element Analysis (FEA) results with mathematical models of spring design from the JIS B 2704-1 standard [1]. Then, it will validate the computational model of a carbon fiber spring (composite materials) considering the experimental results published in the international literature. These validations will allow corroborating the methodology used for the FEA of each of the cases assessed in this study and will ensure the reliability of the results issued.

2. Methodology

The following phases were considered for the numerical analysis of circular cross-section springs with steel, FGM, and composite materials.

- Validation analysis
- Computational models

2.1. Validation Analysis

Some researchers have demonstrated that the mechanical behavior of composite materials, as well as FGM, can be simulated satisfactorily [2]. This research intends to simulate the mechanical behavior of three springs taking into account several experimental research results as well as international standards to demonstrate the reliability of the FEA results in the present investigation. According to JIS B2704-1, the design calculation for steel spring in the case of compression load without initial tension refers to the following equations

Deflection of spring (δ)

$$\delta = \frac{8N_a D^3 P}{Gd^4} \qquad (1)$$

Where:

N_a Number of active coils or number of active turns
D Mean diameter of coil D = (Di + Do)/2; (mm)
P Load (force) acting on spring; (N)
G G modulus of rigidity; (7.85×10^4 N/mm^2 for steel spring)
d Diameter of material (mm)

Spring constant (k)

$$k = \frac{P}{\delta} \qquad (2)$$

Energy stored in spring (U)

$$U = \frac{P\delta}{2} \qquad (3)$$

Eq. (1) will be used to validate the deflection result of the numerical analysis in the case of a steel spring with a circular cross-section. Eqs. (2) and (3) will be used to evaluate the spring performance in each of the three cases assessed in this study.

Composite spring

Chiu C. *et al.* developed an experimental investigation into the mechanical behaviors of helical composite springs made of pre-impregnated fibers fabricated with fibers along with ±45° directions [3]. Then, packed, coiled, and outer braided one layer with resin-impregnated 3K carbon fiber. The present paper will focus only on the “BU” preformed composite bar structure as shown in Fig. 1.

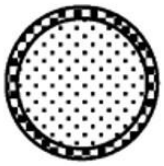

Fig. 1 3K carbon fiber outer braid (one layer): 37.5 cm of length

Experimental results of such research considering a cylindrical helical spring with a square cross-section will be used in this paper only for validation purposes to corroborate the mechanical behavior of the composite spring made of 3k carbon fiber outer braid with a "BU" preformed structure. Fig. 2 and Table 1 show the geometrical dimensions of the square cross-section for the computational model used in the validation of composite spring.

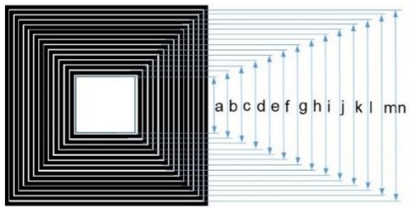

Fig. 2 Geometrical dimensions of the square cross-section for the validation of composite spring

Considering the manufacturing methodology of carbon fiber composite spring [3], Fig. 2 shows the square cross-section compound for a core made of pre-impregnated fibers fabricated with fibers along with ±45° directions with an outer braided one layer of 3K carbon fiber. This 3k carbon fiber lamina with a length of 37.5 cm is coiled 14 times, as shown in Table 1.

Table 1. Geometrical dimensions of the square cross-section for the validation of composite spring

Lamina coiled	Square Cross-Section (Fig. 2)	Side length of square cross-section (mm)	Perimeter (mm)	Carbon Fiber Lamina Total length (cm)
1	a	3.84	15.36	37.5
2	b	4.28	17.12	
3	c	4.72	18.88	
4	d	5.16	20.64	
5	e	5.60	22.40	
6	f	6.04	24.16	
7	g	6.48	25.92	
8	h	6.92	27.68	
9	i	7.36	29.44	
10	j	7.80	31.20	
11	k	8.24	32.96	
12	l	8.68	34.72	
13	m	9.12	36.48	
14	n	9.56	38.24	

The total side length of the square cross-section is 10 mm, after coiling 14 times the 3k carbon fiber lamina according to the description in Table 1 and considering a carbon fiber lamina thickness of 0.22 mm. Table 2 shows the properties of 3k carbon fiber that were used in the numerical simulation.

Table 2: 3k carbon fiber properties

Tow Size k	Filament properties					Minimum carbon content %
	Tensile Strength (GPa)	Young´s Modulus (GPa)	Diameter (mm)	Elongation %	Density g cm-3	
3	**3.75**	**231**	**7.0**	**1.4**	**1.76**	**92**

Source: Morgan P., Carbon Fibers and their composites [4]

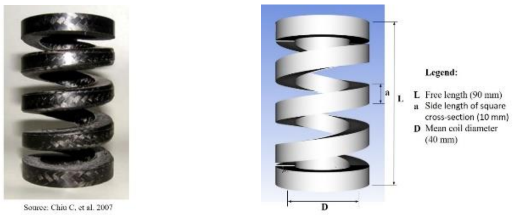

(a) Experimental investigation spring model **(b) Numerical simulation spring model**

Fig. 3 Geometric comparison between the real coil spring and the computational model

Fig. 3a shows the experimental investigation spring model in comparison with the geometrical model developed in the module ACP (pre) from ANSYS Workbench of the composite spring used for validation purposes (Fig. 3b). Considering the maximum compression load in the elastic range of the spring (250 kgf or 2452 N) obtained experimentally by Chiu C. et al. [3]. Fig. 4 shows the boundary conditions and mesh used in the numerical simulation. Spring mesh was refined until achieving the convergence. The final mesh sizing was 0.8 mm (0.031 in) using second-order solid elements.

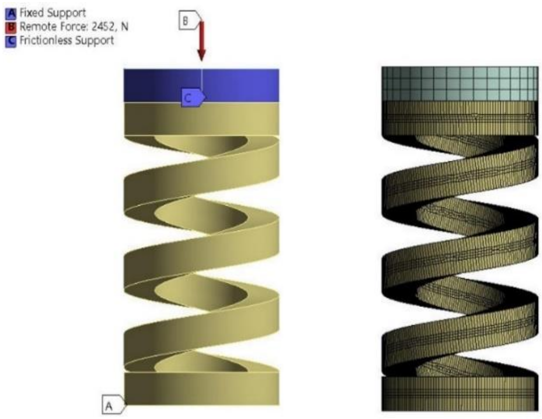

(a) Boundary conditions **(b) Mesh**

Fig. 4 Boundary conditions and mesh of the computational model for validation purpose

Another aspect for validating is the failure load in the elastic range for the composite spring; hence, it will consider the results obtained experimentally by Chiu C. *et al.* [3] related to the failure behavior of this coil spring.

2.2. Computational models

After validating the methodology used for simulating, three geometric models were carried out using ANSYS workbench considering the following general features described in Table 3.

Table 3: General features of computational models [5]

Feature	Computational model		
	1	2	3
Material	Carbon steel C≤0.3%	FGM Carbon Steel C≤0.3% + Al_2O_3)	Composite material (resin epoxy + 3k carbon fibe r)
Shape of spring*	Helical coil both end grounded	Helical coil, both end grounded	Helical coil, both flat end unground
Cross-section shape	Circular	Circular	Circular
Free length (mm)	90	90	90
Cross-section diameter (mm)	10	10	10
Mean coil diameter (mm)	40	40	40
Number of active coils	3.6	3.6	3.6
Type of load applied	Compression	Compression	Compressio n
Type of finite element	2^{nd} order solid Element.	2^{nd} order solid Element.	2^{nd} order solid Element.
Size of element (mm)	0.8	0.8	0.8

2.2.1 Computational model 1

Mechanical and physical properties of the material (carbon steel with C≤0.3%) used for numerical simulation are shown in Table 4.

Table 4. Mechanical and physical properties of carbon steel with C≤0.3% [6]

Property	Value
Density (kg/m^3)	7850
Young´s Modulus (GPa)	201
Poisson´s Ratio	0.3
Tensile Yield Strength (MP a)	250
Compressive Yield Strength (MPa)	250

Fig. 5 depicts the boundary conditions and mesh used in computational model 1. It is highlighted a load compression force of 981 N (220.54 lbf), which is the maximum load in the elastic range.

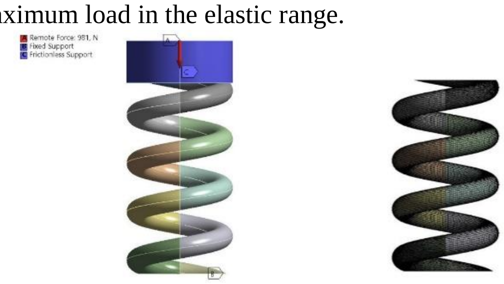

(a) Boundary conditions **(b) Mesh**

Fig. 5 Boundary conditions and mesh of the computational model 1

2.2.2 Computational model 2

Fig. 6 shows the difference in compositions and properties between an ordinary composite material and FGM. There is a distinct interface between metals and ceramics in an ordinary composite material, but not in an FGM. This difference corresponds to the distribution of properties. An ordinary composite material contains a sudden change in properties at the interface, while an FGM presents a gradual change inside it.

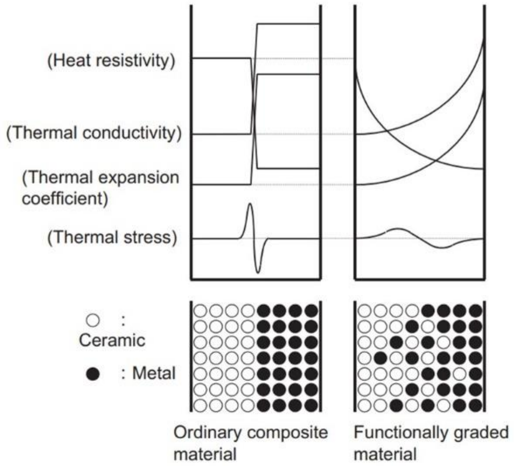

Fig. 6 Material structures and properties of ordinary composite and FGM [7]

For developing the numerical simulation of the FGM compound by carbon steel with less than 0.5% of C in addition to aluminum oxide (Al_2O_3), it was considered the research developed by many researchers [8, 9, 10] to determine the material properties (P) are dependent on the temperature and are expressed in the form:

$$P = P_0\left(\frac{P_{-1}}{T} + 1 + \mathrm{P_1\ T} + \mathrm{P_2\ T^2} + \mathrm{P_3\ T^3}\right) \qquad (4)$$

Where P_0, P_1, P_2, and P_3 are constants in the cubic fit of the material property, and T is the temperature in kelvin. For this paper, T is equivalent to 298 K. Besides, Reddy J. et al. state that to model the material properties of FGM effectively, the properties must be both temperature-dependent and position-dependent [10]. The combination of these functions give rise to the effective material properties of FGMs and is expressed as:

$$P_{eff}(T,\xi) = P_m(T)V_m(\xi) + P_c(T)(1 - V_m(\xi)) \quad (5)$$

Where P_{eff} is the effective material property of FGM; Pm and P_c, are the temperature-dependent properties of the metal and ceramic, respectively; and V_m is the volume fraction of the metal constituent of the FGM. In addition, a simple power-law exponent of the volume fraction distribution is used to provide a measure of the amount of metal in FGMs [10]. For an axisymmetric cylinder, the expression for the volume fraction of ceramic is

$$\mathrm{V_c} = \left(\frac{\mathrm{r - r_i}}{\mathrm{r_0 - r_i}}\right) \qquad (6)$$

Where r_o is the outer radius of the cylinder, r_i is the inner radius, r is the radial coordinate ($r_i \le r \le r_o$), and n is the power-law index ($0 \le n \le \infty$). According to the preceding distribution, the outer surface of the cylinder is ceramic-rich and the inner surface is metal-rich. Table 5 shows the modulus of elasticity of aluminum oxide (Al_2O_3) in Pa, considering Eq. (4). Table 6 shows the Poisson's ratio of aluminum oxide (Al_2O_3), considering Eq. (4).

Table 5. Modulus of elasticity of aluminum oxide [10]

P_0	P_{-1}	P_1	P_2	P_3
349.55x10^{9}	0	-3.853x10^{-4}	4.027x10^{-7}	-1.673x10^{-10}

Table 6. Poisson's ratio of aluminum oxide [10]

P_0	P_{-1}	P_1	P_2	P_3
0.2600	0	0	0	0

For this paper, it was considered a power-law index (n) equivalent to 1. In this case, the mechanical and physical properties of the FGM compound by carbon steel with less than 0.5% of C in addition with aluminum oxide (Al_2O_3) and considering Eqs. (4) to (6) are shown in Table 7.

Table 7. Mechanical and physical properties of FGM

Property	**Value**
Density (kg/m^3)	$7850\left(1-\frac{r}{r_0}\right)+3800\left(\frac{r}{r_0}\right)$
Young´s Modulus (Pa)	$2.01x10^{11}\left(1-\frac{r}{r_0}\right)+3.204x10^{11}\left(\frac{r}{r_0}\right)$
Poisson´s Ratio	$0.3\left(1-\frac{r}{r_0}\right)+0.26\left(\frac{r}{r_0}\right)$
Tensile Yield Strength (Pa)	$2.5x10^{8}\left(1-\frac{r}{r_0}\right)+4x10^{8}\left(\frac{r}{r_0}\right)$
Compressive Yield Strength (Pa)	$2.5x10^{8}\left(1-\frac{r}{r_0}\right)+4x10^{8}\left(\frac{r}{r_0}\right)$

Some researchers developed an algorithm to simulate properties of FGM for the design optimization in a dental implant for bone remodeling [11]. In this sense, and to estimate the mechanical and physical properties, which are position-dependent, was developed an algorithm to simulate this computational model in the ANSYS workbench.

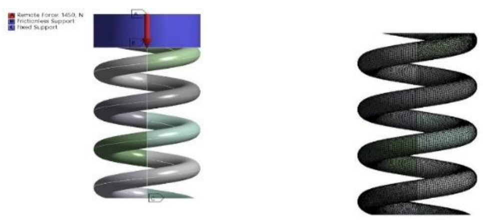

(a) Boundary conditions **(b) Mesh**

Fig. 7 Boundary conditions and mesh of the computational model 2

Fig. 7 depicts the boundary conditions and mesh used in computational model 2. It is highlighted a load compression force of 1450 N (325.97 lbf), which is the maximum load in the elastic range.

2.2.1 Computational model 3

Considering the same methodology explained in section 2.1 about the validation of composite spring simulation, Fig. 8 shows the geometrical dimensions of the circular cross-section for computational model 3.

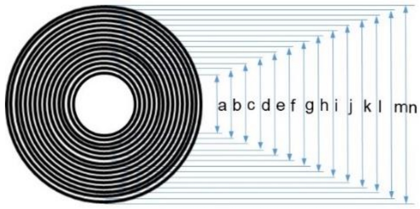

Fig. 8 Geometrical dimensions of the circular cross-section for computational model 3

Table 8 shows the geometrical dimensions of the circular cross-section for computational model 3.

Table 8. Geometrical dimensions of the circular cross-section for computational model 3

Lamina coiled	Circular cross-section (Fig. 8)	Circular cross-section diameter (mm)	Total length of Carbon Fiber lamina (cm)
1	a	3.84	29.5
2	b	4.28	
3	c	4.72	
4	d	5.16	
5	e	5.60	
6	f	6.04	
7	g	6.48	
8	h	6.92	
9	i	7.36	
10	j	7.80	
11	k	8.24	
12	l	8.68	
13	m	9.12	
14	n	9.56	

The final diameter of the circular cross-section is 10 mm, after coil 14 times the 3k carbon fiber lamina according to the description in Table 8 and considering a carbon fiber lamina thickness of 0.22 mm. Table 2 shows the properties of 3k carbon fiber that will use in the numerical simulation. Fig. 9 depicts the boundary conditions and mesh used in computational model 3. It is highlighted a load compression force of 1070 N (240.55 lbf), which is the maximum load in the elastic range.

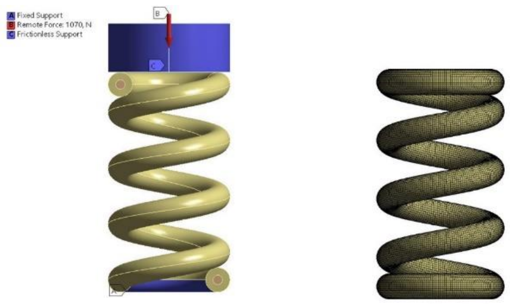

(a) Boundary conditions **(b) Mesh**

Fig. 9 Boundary conditions and mesh of computational model 3

3 RESULTS AND DISCUSSION

3.1. Validation Analysis

Fig. 10 shows the maximum displacement in the elastic range for the carbon steel spring considering a compression load of 981 N (220.54 lbf).

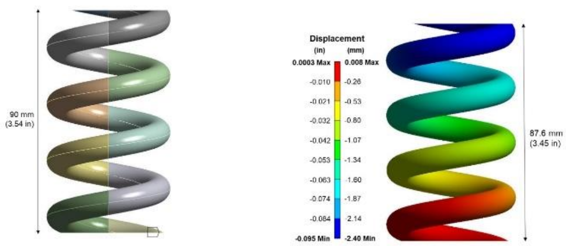

(a) Initial conditions **(b) Final condition**

Fig. 10 Steel spring maximum displacement in the elastic range

Eq. (1) represent the deflection of the spring according to international standard JIS B2704-1 (2009). Considering this Eq. (1), the theoretical maximum deflection in the elastic range for the carbon steel spring is 2.3 mm, and the FEA result in Fig. 10 shows a maximum displacement equivalent to 2.4 mm, in consequence, the relative error is 4.19%. Hence, results about displacement demonstrate that numerical simulation of the steel spring can represent very well the spring theoretical behavior. Fig. 11 shows the maximum displacement in the elastic range for the composite spring with a square cross-section.

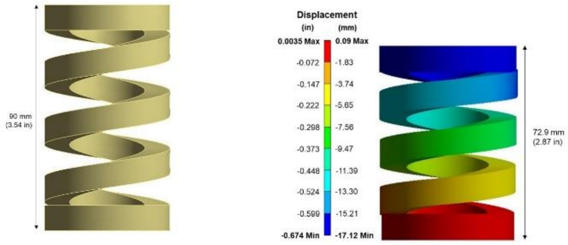

(a) Initial conditions **(b) Final condition**

Fig. 11 Composite spring maximum displacement in the elastic range

The maximum deflection for the composite spring during the experiment in the elastic range is 16.23 mm [3] and the FEA result in Fig. 11 shows a maximum displacement equivalent to 17.12 mm, hence the relative error is 5.48%. When it is compared the experimental behavior of failure (right picture in Fig. 12) with results obtained by FEA (left picture in Fig. 12), it can be noticed that there is some correspondence in the failure location.

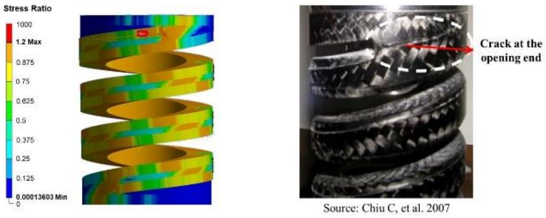

(a) Numerical simulation of failure **(b) Experimental behavior of failure**

Fig. 12 Comparison of failure between FEA simulation and experimental behavior of composite spring

The maximum stress ratio (1.2) in FEA results match the experimental location of a crack at the opening end of the coil spring. With this compressive load (1452 N), the spring in the numerical simulation exhibits an orange color in most coils of spring that represent a stress ratio near to one, being the value of 1 the limit of the stress ratio for the failure in the elastic range. Stress ratio values equal to or more than one represents a failure by yield strength. In consequence, results about not only displacement but also failure behavior demonstrate that numerical simulation of the composite spring can represent very well the composite spring behavior during experimental investigation.

3.2. Computational models

3.2.1 Computational model *1*

Fig. 10 shows the steel spring maximum displacement in the elastic range, and this displacement was validated with Eqs. 1 and 2 that represents the theoretical behavior. Fig. 13 exhibits the stress ratio obtained in the numerical simulation, considering that stress ratio equivalent or more than 1 represents the failure in the elastic range of the material. In this case, Fig. 13 shows a maximum stress ratio equivalent to 1.025, which means that the material reaches the yield strength; hence, the compression load used in this numerical simulation (981 N) is considered as the maximum load in the elastic range.

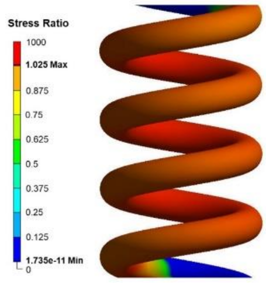

Fig. 13 Failure at maximum displacement in the elas tic range for computational model 1

3.2.2 Computational model 2

Fig. 14 shows the FGM spring maximum displacement in the elastic range. It can be noticed a maximum displacement equivalent to 2.48 mm considering a compressive load of 1450 N (325.97 lbf).

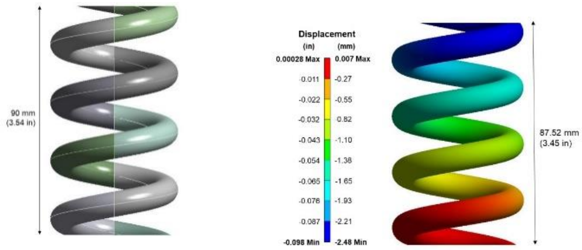

(a) Initial conditions **(b) Final condition**

Fig. 14 Maximum displacement in the elastic range for computational model 2

Fig. 15 shows the stress ratio obtained in the numerical simulation, with a maximum stress ratio equivalent to 1.03, it means that the material reaches the yield strength; hence, the compression load used in this numerical simulation (1450 N) is considered as the maximum load in the elastic range.

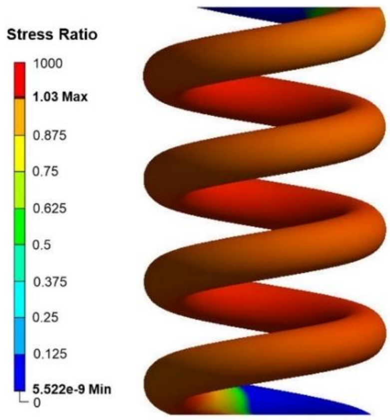

Fig. 15 Failure at maximum displacement in the elas tic range for computational model 2

3.2.3 Computational model 3

Fig. 16 exhibits the composite spring maximum displacement in the elastic range. It can be noticed a maximum displacement is equivalent to 15.07 mm (0.59 in) considering a compressive load of 1070 N (240.55 lbf).

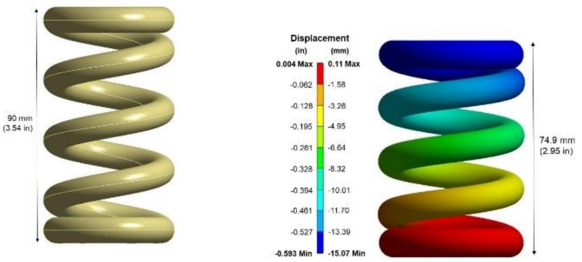

(a) Initial conditions (b) Final condition

Fig. 16 Maximum displacement in the elastic range for computational model 3

Fig. 17 shows the stress ratio obtained in the numerical simulation, obtaining a maximum stress ratio equivalent to 1.05; it means that the material reaches the yield strength; hence, the compression load used in this numerical simulation (1070 N) is considered as the maximum load in the elastic range.

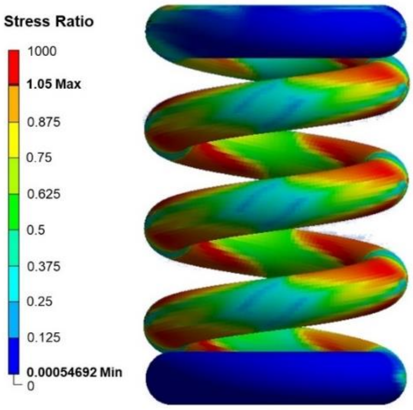

Fig. 17 Failure at maximum displacement in the elas tic range for computational model 3

Table 9 shows the performance comparison between these three computational models, which will help to better understand how new development in materials such as FGM and composite can enhance the capability and potential use of springs.

Table 9. Comparison of spring performance

Computational mode l	**1 (Plain Steel)**	**2 (FGM)**	**3 (Compo site)**
Failure load (N)	981	1450	1070
Deflection □ (mm)	2.40	2.48	15.07
Spring constant k (N /mm)	408.75	584.68	71.00
Weight of spring (g)	307.0	187.7	74.6
Energy stored in spri ng U (J)	1177.20	1798.00	8052.45
Specific energy store d in spring (J/g)	3.83	9.58	108.07

As shown in Table 9, springs made of FGM and composite outperform springs made of carbon steel in some characteristics. Regarding load-to-failure performance, an FGM spring outperforms a carbon steel spring 1.48 times, while a carbon fiber spring outperforms its carbon steel counterpart by 1.1 times. Regarding weight, and for industrial applications that require it, such as in the manufacturing of vehicles and automobiles [12], this performance characteristic also shows its advantages for FGM and composite springs. As shown in Table 9, the weight of an FGM spring represents only 61% of the mass of a carbon steel spring, while its similar one made of composite has a weight equivalent to 24% of the weight carbon steel spring. Another favorable feature is about the energy storage in the coil spring, where again both springs, FGM and composite, outperform their carbon steel counterpart by 1.53 times and 6.84 times, respectively. In the same sense, the characteristic about specific energy stored in the coil spring that relates the energy stored in the spring with the weight of the spring demonstrates that a composite spring can store more energy per mass unity, 11.3 times more than an FGM spring and 28.2 times more than a steel spring. On the other hand, for applications that require high stiffness or higher spring constant, the best option is an FGM spring, followed by a carbon steel spring, and at last, a composite material spring. This characteristic intrinsically linked to the deflection of the spring is modifiable in a composite material spring by selecting laminates of carbon fiber with mechanical properties superior to those used in the present work [4].

4 CONCLUSIONS

Three computational models were carried out to compare the spring performance considering three different kinds of materials: carbon steel, FGM compound by carbon steel + aluminum oxide, and composite material. Validation of these computational models was confirmed considering international standards and international publications. The results of this work show that some feature performances of compression springs made of carbon steel are improved when using FGM and composite materials. Enhanced capabilities include higher load to failure (1.48 times in an FGM spring and 1.1 times in a composite spring), as well as increased energy storage (1.53 times in an FGM spring and 6.84 times in a composite spring) and less weight (representing 61% in weight in an FGM spring and 24% in a composite spring)

REFERENCES:

[1] JIS B 2704-1, Japanese Industrial Standard, “Coil springs- Part 1: Basic calculation methods on helical compression and extension springs” (2009).

[2] Almeida C., Albino J., Menezes I., Paulino G., “Geometric nonlinear analyses of functionally graded beams using a tailored Lagrangian formulation”. *Elsevier Journal. Mechanics Research Communications*, (2011) **38**(8)553-559. https://doi:10.1016/j.mechrescom.2011.07.006

[3] Chiu C., Hwan C., Tsai H., Lee W., “An experimental investigation into the mechanical behaviors of helical composite springs”. *Elsevier Journal. Composite Structures*, (2007), **77**(3), 331-340. https://doi.org/10.1016/j.compstruct.2005.07.022

[4] Morgan P., Carbon Fibers and their Composites. Taylor &Francis Group. ISBN-10: 0-8247-0983-7, (2005) Boca Raton, FL, USA.

[5] JIS B 2704-2, Japanese Industrial Standard, “Coil Springs-Part 2: Expression of the specification on helical compression springs” (2009).

[6] ASME, “ASME Boiler & Pressure Vessel Code”,

Section II Part D, Properties-Material ASME, (2017), New York. USA.

[7] Somiya S., (2013), Handbook of Advanced Ceramics. Materials, Applications, Processing, and Properties. Academic Press. http://dx.doi.org/10.1016/B978-0-12-385469-8.00001-0

[8] Naebe M., Shirvanimoghaddam K., "Functionally graded materials: A review of fabrication and properties". *Elsevier Journal. Applied Materials Today* **5**(2016), 223-245.

[9] https://doi.org/10.1016/j.apmt.2016.10.001

[10] Shen H., Functionally Graded Materials, Nonlinear Analysis of Plates and Shells. CRC Press. Taylor & Francis Group, (2009), ISBN-13: 978-1-4200-9256-1.

[11] Reddy J. N., Chin C. D., "Thermomechanical Analysis of Functionally Graded Cylinders and Plates". Taylor &Francis Group. Journal of Thermal Stresses, **21**(1998), 593-626. http://dx.doi.org/10.1080/01495739808956165

[12] Lin D., Li Q., Li W., Zhou S., Swain M., "Design optimization of functionally graded dental implant for bone remodeling". *Elsevier Journal. Composites Part B* **40**(2009), 668-675. https://doi:10.1016/j.compositesb.2009.04.015

[13] Sancaktar E., Gratton M., "Design, analysis, and optimization of composite leaf springs for light vehicle applications". *Elsevier Journal. Composite Structures* **44**(1999), 195-204. https://doi.org/10.1016/S0263-8223(98)00136-6

[14] Choi B. L., Choi B. H., "Numerical method for optimizing design variables of carbon-fiber-reinforced epoxy composite coil springs". *Elsevier Journal. Composites Part B: engineering*. **82**(2015), 42-49 https://doi.org/10.1016/j.compositesb.2015.08.005

[15] Jiang Q., Qiao Y., Zhao F., Pan Z., Wu X., Wu L., Fu., H, "Composite helical spring with skin-core structure: Structural design and compression property evaluation". *Wiley Journal. Polymer Composites*. 2020; 1–13. https://doi.org/10.1002/pc.25901

[16] Rashad M., Wahab M., Yang T.Y., "Experimental and numerical investigation of RC sandwich panels with helical springs under free air blast loads" *Techno Press Journal. Steel and Composite Structures*, (2019)m **30**(3), 217-230. http://dx.doi.org/10.12989/scs.2019.30.3.217

[17] Yang P., Van Dyke S., Elhajjar R., "An investigation into the mechanics of fiber reinforced composite disk springs" *Techno Press Journal. Steel and Composite Structures*, , (2015), **18**(3), 775-791. http://dx.doi.org/10.12989/scs.2015.18.3.775